EURASIAN PHYSICAL TECHNICAL JOURNAL

2025, Volume 22, No. 3 (53)

https://doi.org/10.31489/2025N3/48-54

Received: 16/02/2025 Revised: 12/08/2025 Accepted: 25/09/2025 Published online: 30/09/2025

Research Article

UDC 535.37

SYNTHESIS OF SILVER NANOPARTICLES AND THEIR INFLUENCE ON THE FLUORESCENCE AND ABSORPTION OF ANTHRACENE

Yusupova Zh.B.

Institute of Molecular Nanophotonics, Karaganda Buketov University, Karaganda, Kazakhstan
Corresponding author: yusupova-zh@mail.ru

Abstract. *The synthesis process of island silver films was investigated, with a focus on the role of solution pH as a key parameter for successful film formation. It was determined that the optimal pH for effective synthesis is 8. The results of particle distribution analysis by Feret diameter, performed using the ImageJ software, are also presented. The distribution histogram confirmed that the chemically deposited film is of high quality. The developed synthesis method enables the fabrication of silver nanoparticle films with tailored properties. The influence of the synthesized silver films on the luminescent properties of anthracene was studied, highlighting their potential applications in photonics and sensor technologies.*

Keywords: island films, silver nanoparticles, anthracene, pH, ImageJ.

1. Introduction

In recent years, there has been rapid development in research devoted to localized surface plasmon resonance (LSPR) of metallic nanoparticles (NPs), which has contributed to the emergence of advanced analytical techniques and technological solutions [1]. When interacting with a light source, NPs made of metals such as silver, gold, copper, or aluminum exhibit collective oscillations of free electrons, leading to a significant enhancement of the electromagnetic field in their vicinity. It has been reported that the electric field intensity near such nanoparticles can increase by a factor of up to 10^4 [2]. Fluorophore or analyte molecules located in close proximity to these NPs experience intense external influence, which accelerates photocatalytic reactions [3], enhances luminescence, and facilitates surface-enhanced Raman scattering (SERS) [4, 5].

Plasmon-enhanced fluorescence is a well-studied phenomenon. Research shows that the fluorescence of dye molecules can either be enhanced or quenched depending on the distance between the nanoparticles and the emitting species, as well as their mutual dipole orientation. This effect finds applications in devices based on the control of radiative processes. The LSPR of metallic nanoparticles influences the relaxation dynamics of photoexcited emitters through the Purcell effect [6, 7] and also contributes to the reduction of the lasing threshold in dye-based lasers. Plasmonic effects are employed in the development of materials with tailored optical properties, in sensing technologies, and in optoelectronic devices [8, 9].

Particular interest lies in the influence of plasmons on long-lived luminescence processes associated with spin effects. Long-lived triplet states are crucial for fundamental processes and have significant practical relevance. For instance, prolonged emission of molecular probes is used in bioimaging to improve the signal-to-noise ratio. Triplet states are also utilized in photosynthetic systems for the generation of singlet oxygen, which is essential in photodynamic therapy, antibacterial treatments, and in the treatment of skin and

respiratory diseases. Moreover, triplet states of organic compounds find applications in OLED technologies, solar cells, and transistors [10, 11].

This article presents the results of silver nanoparticle film synthesis, surface analysis, and measurement data demonstrating the positive effect of plasmonic enhancement on the luminescent properties of anthracene.

2. Experimental section and measurements details

Anthracene was selected as the luminescent molecule and was purchased from Sigma-Aldrich. For the synthesis of silver island films, the following reagents were used: $AgNO_3$, NaOH, NH_4OH, D-glucose, and polyvinyl alcohol (PVA), all of analytical grade (Sigma-Aldrich). Ultrapure water obtained using the Smart S15 UVF system (Drawell) was used for sample preparation.

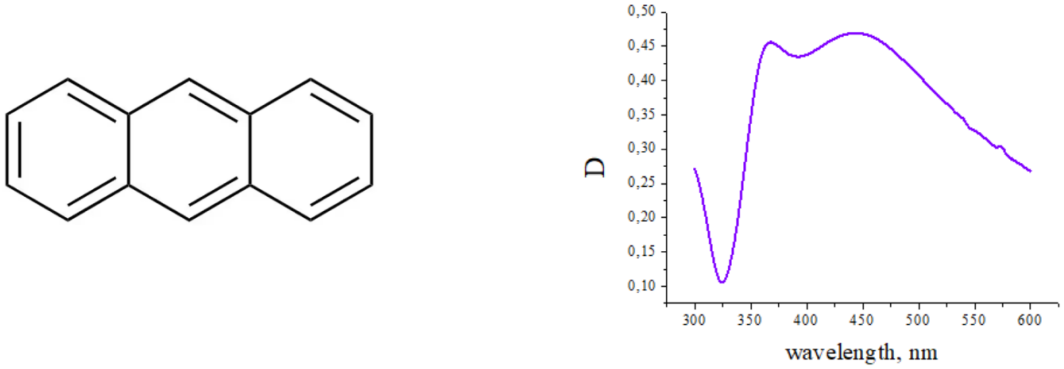

a) b)

Fig. 1. Molecular structure (a) of the studied compound and the absorption spectrum (b) of the silver island film (SIF).

The chemical deposition procedure used for the fabrication of silver island films (SIFs) was based on the method described in [12]. The synthesis involves several key steps (fig. 2):

Fig. 2. Key steps of synthesis process

When the synthesis is carried out correctly, it is assumed that the process can be controlled. Key factors that influence the process include the pH of the solution and the amount of reducing agent.

A 5% sodium hydroxide (NaOH) solution is added to the silver nitrate ($AgNO_3$) solution (process 1), resulting in the formation of a brown precipitate — silver oxide (Ag_2O).

$$2AgNO_3 + 2NaOH = Ag_2O\downarrow + 2NaNO_3 + H_2O \quad (1)$$

Next, ammonium hydroxide (NH_4OH) was added to the solution (process 2), dissolving the silver precipitates and forming an ammonia complex. A 25% solution of ammonium hydroxide was used for the synthesis. Previous studies have shown a relationship between the size of silver nanoparticles and the concentration of ammonia, as well as the pH of the medium during the reduction process.

When ammonium hydroxide was introduced into the silver nitrate solution, the pH initially reached 10, indicating an alkaline environment typical for ammonia solutions. However, over time, the pH gradually decreased to 8 and continued to lower, suggesting the release of ammonium ions (NH_4^+) and their reaction with water. This may indicate a weakening of the buffer capacity of the solution, affecting the pH

.

stabilization during synthesis. The decrease in pH accelerates the synthesis of silver nanoparticles and facilitates the formation of high-quality silver films. The possible reason for the acceleration of the reaction is the optimal conditions for the silver-ammonia complex and more efficient reduction of silver at pH 8 [13]. Furthermore, continuous mechanical stirring on a magnetic stirrer might have enhanced the contact between the components and accelerated the chemical reactions, which could also have contributed to the further reduction of pH.

$$Ag_2O + 4NH_4OH \rightarrow 2\left[Ag(NH_3)_2\right]OH + 3H_2O \quad (2)$$

The transparent solution is placed in a cooling bath to cool down to a temperature of -5°C. This step is necessary to ensure that the synthesis of silver nanoparticles occurs slowly until the temperature rises to 30°C. Under these conditions, the reduction of silver nanoparticles proceeds gradually and uniformly. Once the solution reaches the low temperature, the substrates are immersed, and glucose is added (process 3), which aids in the reduction of silver.

$$2\left[(NH_3)_2OH + C_2H_{12}O_6 \rightarrow 2Ag\downarrow + 4NH_3 + C_2H_{12}O_7 + H_2O\right] \quad (3)$$

After the addition of glucose, the pH level remained at 8, which is an ideal condition for synthesis. The solution was then heated to 30°C. Once the temperature reached 14-16°C, the solution began to change color from transparent to golden-yellow. At temperatures between 18-19°C, the solution turned dark green. At this stage, the films obtained had an optical density of 0.3-0.5. If the temperature was allowed to rise to 21-25°C, the film would compact further, and the optical density would increase to 0.4-0.8. After the synthesis was completed, the subsequent steps were carried out according to the procedure described in the literature [12]. This study refined the key stages of the synthesis, particularly the conditions for the reduction of silver nanoparticles. The annealing was performed at 200°C for 90 minutes.

Figure 3 presents images of silver nanoparticles, the absorption spectrum, and the particle size distribution histogram based on Feret's method. The SEM image was obtained using a Helios 5 CX scanning electron microscope. According to the data from the scanning electron microscope, the average particle size was found to be 95±30 nm. These films are characterized by the presence of an absorption band in the visible region of the spectrum (see Figure 2). The polymer coatings with an anthracene concentration of 1×10^{-3} mol/l were applied using the drop-casting method.

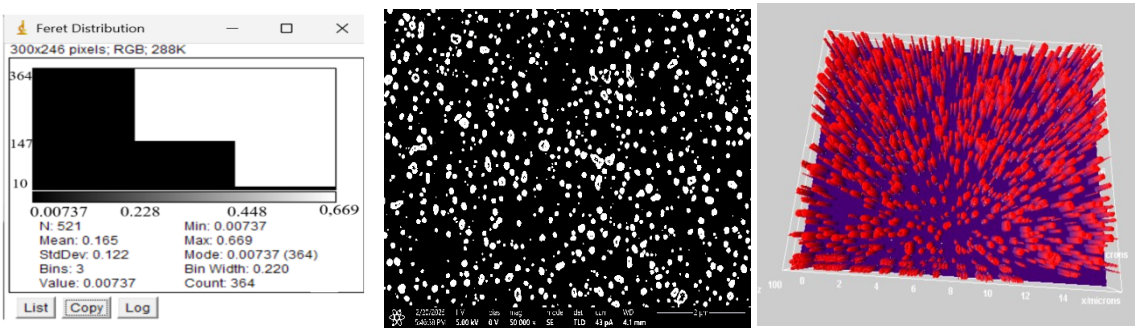

a) b) c)

Fig. 3. Histogram (a), SEM image (b), and 3D image of the particles (c).

For further investigation of the film surface, the ImageJ software was used to analyze the images obtained via scanning electron microscopy (SEM). The program provided data on the distribution of particles based on Feret's diameters. However, it is important to note that while ImageJ effectively analyzes SEM images, the results may depend on the size and orientation of the particles, which can affect their visibility and measurement accuracy. Therefore, SEM remains the primary method for detailed observation and analysis of particle structure.

In the process of analyzing 521 particles found in an image measuring 16 × 11.40 μm, the following results were obtained: for each particle, the Feret diameter (the largest distance between two points on the outer boundary of the particle) was measured. The minimum Feret value was 0.00737 μm, and the maximum

was 0.669 μm, indicating a wide range of particle sizes. The average particle diameter was 0.165 μm, and the standard deviation was 0.122 μm, suggesting significant variability in particle sizes. The modal value for the particles was 0.00737 μm, which represents the most frequently occurring size.

The histogram of particle distribution showed that 364 particles have a size corresponding to the bin of 0.00737 μm (the most frequent value), 124 particles correspond to the bin of 0.228 μm, 10 particles correspond to the bin of 0.448 μm, and fewer than 10 particles have a size around 0.669 μm. The bin size in the histogram was 0.220 μm, which defines the resolution of the histogram and allows for the assessment of the distribution of particle sizes.

The program determines the particle sizes in pixels/microns, which is incorrect to directly compare these units with the actual particle sizes in the film. A total of 521 particles were involved in the analysis, and the program determined that 73% showed smaller sizes, 25% showed medium sizes, and 2% showed large sizes. Based on the obtained results, it can be concluded that 73% of the particles correspond to the average size of 95±30 nm, which indicates the high quality of the synthesis process.

Additionally, the 3D image (fig.2, (c)) was generated based on SEM images using the ImageJ software, which allows surface topography visualization. Specifically, the "3D Surface Plot" module was used to create a volumetric reconstruction based on the brightness contrast of the image.

Particles with a diameter in the range of 50–100 nm are considered high-quality for various applications such as sensors, catalysts, and optical materials. According to research, particle size within this range is optimal for achieving high performance in these areas due to their enhanced optical, chemical, and catalytic properties. Silver particles with sizes ranging from 50–150 nm can effectively interact with the surrounding environment, especially in the context of plasmonic resonance. This interaction leads to fluorescence enhancement, which is particularly important for the application of nanoparticles in photonics and other optical devices [14, 15].

The absorption spectra of the samples were recorded using a Cary-300 spectrophotometer (Agilent Technologies). Fluorescent and long-lived luminescent spectra were recorded using an Eclipse spectrofluorometer (Agilent Technologies). In the case of long-lived luminescence, the spectra were recorded with a delay of 300 μs after the pulse from the xenon lamp.

Fluorescence decay kinetics measurements were conducted using the time-correlated single-photon counting (TCSPC) method with an FLS1000 spectrometer (Edinburgh Instruments). Excitation was performed with a laser at a wavelength of 375 nm and a pulse duration of 120 ps. The fluorescence lifetime analysis was performed using Fluoracle software (Edinburgh Instruments). For the registration of long-lived luminescence decay kinetics, the FLS1000 spectrometer was also used. The sample was excited at 362 nm using an Nd:YAG laser system LQ529, equipped with an optical parametric generator LP604 and a second-harmonic generator LG350 (SolarLS). To prevent contact with oxygen, the samples were vacuumed in an Optistat DN-V cryostat (Oxford Instruments). All measurements were carried out at a temperature of 293 K.

3. Results and Discussion

The absorption spectrum of silver nanoparticles (Figure 4, curve 3) in the film shows a broad band with maxima at 368 and 444 nm, which coincides well with the absorption and fluorescence spectra of anthracene (Figure 4, curves 1, 2). This indicates that the conditions for the manifestation of plasmon resonance in the photonics of lumophore molecules are met [16-18]. The absorption maxima of anthracene occur at 362 nm, and the fluorescence maxima occur at 404 nm.

Illustration 5 shows the influence of silver nanoparticles on the optical properties of anthracene. The silver nanoparticles contributed to a 1.2-fold increase in the absorption intensity of anthracene, and the fluorescence intensity of anthracene increased by 2.5 times. An increase in the electric field intensity near the surface during the excitation of surface plasmons leads to an increase in the intensity of fluorescence spectra [19].

Figure 6 shows the fluorescence decay kinetics of anthracene (1) and in the presence of silver nanoparticles (2). The presence of silver nanoparticles increased the fluorescence intensity and also shortened the fluorescence lifetime by a factor of 1.3. In silver island films, an increase in the decay rate of fast fluorescence of molecules is often observed [20, 21]. The reason for this phenomenon lies in the interaction between the electrons of silver particles and the fluorophore molecule.

.

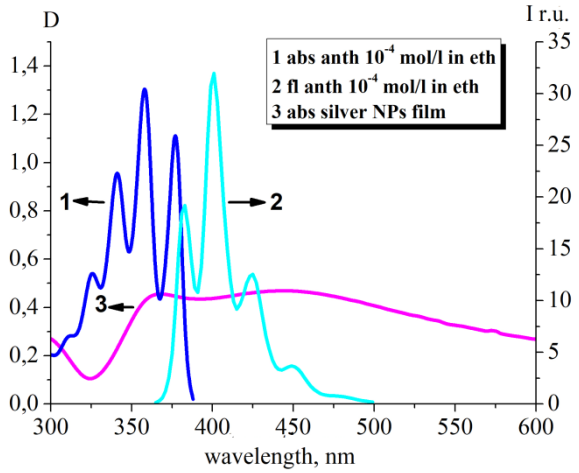

Fig. 4. Absorption and fluorescence spectra of anthracene (C = 10^{-4} mol/L in ethanol) and the absorption spectrum of the silver nanoparticle film.

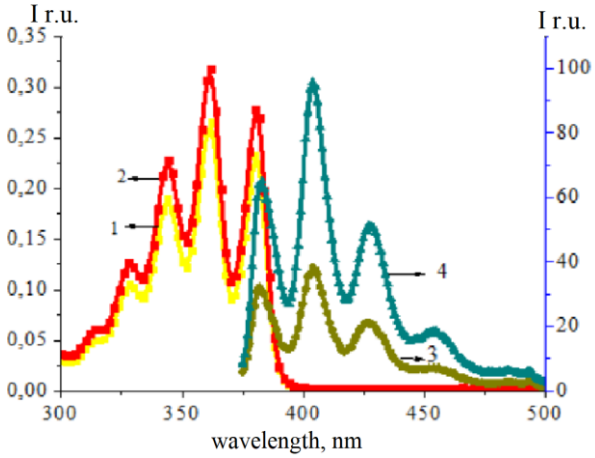

Fig. 5. Influence of silver nanoparticles on the absorption spectra (1,2) and fluorescence spectra (3,4) of anthracene in PVB films (C = 10^{-3}, 4% PVB). Curves 1 and 3 represent anthracene films on quartz substrates; curves 2 and 4 represent anthracene on the surface of silver nanoparticles

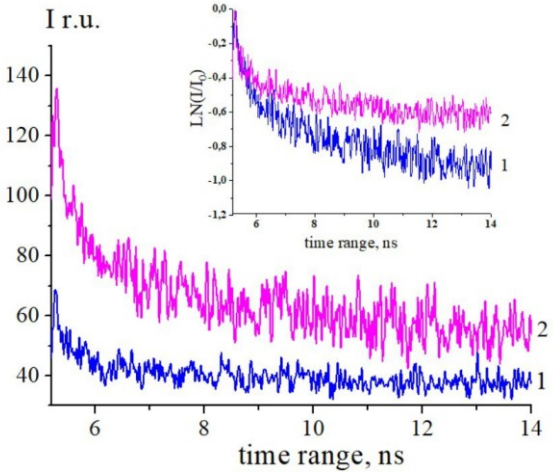

Fig. 6. Kinetics of fast fluorescence of anthracene (1) and in the presence of silver nanoparticles (2)

The process of transition between the excited and ground states of the fluorescent molecule is accelerated, which leads to a reduction in the fluorescence lifetime, an increase in its quantum yield, and a rise in the proportion of non-radiative processes in the transitions from the excited state [20-23].

The spectral characteristics of anthracene on quartz and in the presence of silver nanoparticles are summarized in Table 1. It can be seen that silver island films enhance the fluorescence intensity and influence the excited-state lifetime.

Table 1. Spectral data of anthracene in the presence of silver nanoparticles

	D	λ_{ex} *(nm)*	I_{fl}	λ_{em} *(nm)*	τ *(ns)*
Anthracene on Q	0,26	362	37	404	4,7
Anthracene on SIF	0,31	362	94	404	3,7

As can be seen from Table 1, the optical density (D) of anthracene on silver island films (SIF) shows a slight increase compared to quartz, rising from 0.26 to 0.31, indicating enhanced absorption properties. More significantly, the fluorescence intensity (I_f) increases by approximately 2.5 times, demonstrating a strong enhancement of emission in the presence of silver nanoparticles. Concurrently, the fluorescence lifetime (τ) decreases from 4.7 ns to 3.7 ns, an approximately 1.3-fold reduction, which suggests an acceleration of radiative decay processes. This phenomenon, known as plasmon–fluorophore coupling, arises from the interaction between the localized surface plasmons of silver nanoparticles and anthracene fluorophores, resulting in enhanced emission intensity and reduced fluorescence lifetime. These results underline the important role of silver nanoparticles in modifying the photophysical properties of anthracene, with potential applications in sensing and optoelectronic devices [8, 9].

4. Conclusions

As a result of the conducted research, island silver films were synthesized using the reduction method in a silver nitrate solution. Special attention was given to the role of the solution pH as a key parameter influencing the nanoparticle synthesis process. The use of ammonium hydroxide helped stabilize the pH at a level optimal for the formation of silver nanoparticles. The particle distribution histogram by Feret, obtained using the ImageJ program, showed that the film synthesized by the chemical deposition method was relatively homogeneous, with the majority of particles having an average size of silver nanoparticles.

The study of the influence of the synthesized island silver films on the luminescent properties of anthracene showed that the presence of silver nanoparticles leads to a significant increase in the fluorescence intensity of anthracene by 2.5 times. This enhancement is associated with the plasmon resonance effect and the intensification of the electric field near the surface of the nanoparticles. The lifetime of the excited state of anthracene molecules near silver nanoparticles is reduced by 1.3 times, confirming the impact of the plasmon effect on the transition between excited and ground states.The obtained results demonstrate that silver nanoparticles can effectively modify the fluorescence of anthracene molecules, opening up prospects for further research in the fields of photonics, sensor technologies, and biomedicine.

This study emphasizes the importance of optimizing nanoparticle synthesis conditions and their interaction with fluorophore molecules, which could form the basis for the development of new materials with enhanced optical characteristics.

Funding

This research is funded by the Science Committee of the Ministry of Science and Higher Education of the Republic of Kazakhstan (Grant No. AP23490195).

References

1. Novotny L., Hecht B. (2006) *Principles of nano-optics* (p. 539). Cambridge University Press. https://doi.org/10.1017/CBO9780511813535

2. Harrison R.K., Ben-Yakar A. (2010) Role of near-field enhancement in plasmonic laser nanoablation using gold nanorods on silicon substrate. *Optics Express,* 18**,** 22556–22571. https://doi.org/10.1364/OE.18.022556

.

3. Omarova G.S., Serikov T M., Seliverstova E.V., Auzhanova A.A., Ibrayev N.Kh. (2024) Influence of plasmon effect on the sensitization of titanium dioxide by dye molecules. *Eurasian Physical Technical Journal,* 21(47), 49–56. https://doi.org/10.31489/2024No1/49-56

4. Xiao X.H., Rodriguez R.S., Haynes C.L., Ozaki Y., Zhu B. (2021) *Surface-enhanced Raman spectroscopy***.** Springer Nature. https://doi.org/10.1038/s43586-021-00083-6

5. Brosseau C.L., Colina A., Perales-Rondon J.V., Wilson A.J., Joshi P.B., Ren B., Wang X. (2023) Electrochemical surface-enhanced Raman spectroscopy. *Nature Reviews,* 3(79). https://doi.org/10.1038/s43586-023-00263-6

6. Krivenkov V., Samokhvalov P., Nabiev I., Rakovich Y.P. (2020) Synergy of excitation enhancement and the Purcell effect for strong photoluminescence enhancement in a thin-film hybrid structure based on quantum dots and plasmon nanoparticles. *Journal of Physical Chemistry Letters***,** 11(19), 8018–8025. https://doi.org/10.1021/acs.jpclett.0c02296

7. Kumbhakar P., Biswas S. (2019) Resonance energy transfer-assisted random lasing in light-harvesting bio-antenna enhanced with a plasmonic local field. *RSC Advances,* 9(65), 37705–37713. https://doi.org/10.1039/c9ra08166f

8. Ibrayev N.K., Aimukhanov A.K. (2019) Influence of plasmon resonance in silver nanoparticles on the properties of stimulated emission of 1,3,5,7,8-pentamethyl-2,6-diethylpyrromethene-difluoroborate molecules in film of porous aluminum oxide. *Optics and Laser Technology***,** 115, 246–250. https://doi.org/10.1016/j.optlastec.2019.02.040

9. Seliverstova E.V., Ibrayev N.K. (2016) Plasmon-enhanced stimulated emission of chromene dye. *Journal of Physics: Conference Series***,** 735, 012018. https://doi.org/10.1088/1742-6596/735/1/012018

10. Temirbayeva D., Ibrayev N., Seliverstova E., Kudinova M., Ishchenko A. (2022) Plasmon effect on triplet-singlet energy transfer in the dye-doped Langmuir-Blodgett films. *Bulletin of the Karaganda University: Physics Series,* 4(108), 6–13. https://doi.org/10.31489/2022ph4/6-13

11. Seliverstova E.V., Ibrayev N.K., Zhumabekov A.Z. (2020) The effect of silver nanoparticles on the photodetecting properties of the TiO2/graphene oxide nanocomposite. *Optics and Spectroscopy*, 128**,** 1449–1457. https://doi.org/10.1134/s0030400x20090192

12. Kadir A., Leonenko Z., Lakowicz J.R., Geddes C.D. (2005) Annealed silver-island films for applications in metal-enhanced fluorescence: Interpretation in terms of radiating plasmons. *Journal of Fluorescence,* 15(5), 643–654. https://doi.org/10.1007/s10895-005-2970-z

13. Krutyakov Y.A., Kudrinsky A.A., Olenin A.Yu., Lisichkin G.V. (2008) Synthesis and properties of silver nanoparticles: Achievements and prospects. *ChemInform,* 77(3). https://doi.org/10.1002/chin.200835228

14. Liao D.L., Liao B.Q. (2007) Shape, size and photocatalytic activity control of TiO2 nanoparticles with surfactants. *Journal of Photochemistry and Photobiology A: Chemistry, 187*, 363–369. https://doi.org/10.1016/j.jphotochem.2006.11.003

15. Zhan C., Yi J., Hu S., et al. (2023) Plasmon-mediated chemical reactions. *Nature Reviews Methods Primers***,** 3(12). https://doi.org/10.1038/s43586-023-00195-1

16. Stranik O., McEvoy H. M., McDonagh C., MacCraith B.D. (2005) Plasmonic enhancement of fluorescence for sensor applications. *Sensors and Actuators B: Chemical, 107*(1), 148–153. https://doi.org/10.1016/j.snb.2004.08.032

17. Agrawal N., Saxena R., Kumar S. (2022) Recent advancements in plasmonic optical biosensors: A review. *ISSS Journal of Micro and Smart,* 11**,** 31–42. https://doi.org/10.1007/s41683-021-00079-0

18. Deng W., Goldys E.M. (2012) Plasmonic approach to enhanced fluorescence for applications in biotechnology and the life sciences. *Langmuir,* 28, 10152–10163. https://doi.org/10.1021/la300332x

19. Stranik O., Nooney R., McDonagh C., MacCraith B.D. (2007) Optimization of nanoparticle size for plasmonic enhancement of fluorescence. *Plasmonics, 2***,** 15–22. https://doi.org/10.1007/s11468-006-9020-9

20. Lakowicz J.R., Geddes C.D. (2005) Enhanced lanthanide luminescence using silver nanostructures: Opportunities for a new class of probes with exceptional spectral characteristics. *Journal of Fluorescence***,** 15**,** 53–59. https://doi.org/10.1007/s10895-005-0213-y

21. Lakowicz J.R., Maliwal B.P., Malicka J., Gryczynski Z., Gryczynski I. (2002) Effects of silver island films on the luminescent intensity and decay times of lanthanide chelates. *Journal of Fluorescence,* 12**,** 431–437. https://doi.org/10.1023/A:1021318127519

22. Lee I.-Y.S., Suzuki H., Ito K., Yasuda K. (2004) Surface-enhanced fluorescence and reverse saturable absorption on silver nanoparticles. *Journal of Physical Chemistry B***,** 108(50), 19368–19372. https://doi.org/10.1021/jp0471554

23. Aslan K., Holly P., Geddes C.D. (2006) Metal-enhanced fluorescence from silver nanoparticle-deposited polycarbonate substrates. *Journal of Materials Chemistry,* 16**,** 2846. https://doi.org/10.1039/B604650A

AUTHORS' INFORMATION

Yusupova, Zhanat Bahtierovna – PhD student, Institute of Molecular Nanophotonics, Buketov Karaganda University, Karaganda, Kazakhstan; Scopus ID: 57204979523, ORCID iD: 0009-0000-6178-5313; yusupova-zh@mail.ru